Specificity Determinants of Recruitment Peptides Bound to Phospho-CDK2/Cyclin A[†,‡]

Edward D. Lowe,[§] Ivo Tews,[¶] Kin Yip Cheng,[§] Nick R. Brown,[§] Sheraz Gul,[¶] Martin E. M. Noble,[§] Steven J. Gamblin,[¶] and Louise N. Johnson*[,§]

Laboratory of Molecular Biophysics, University of Oxford, Rex Richards Building, Oxford OX1 3QU, UK, and Protein Structure Division, National Institute for Medical Research, The Ridgeway, Mill Hill, London NW7 1AA, UK

Received September 23, 2002; Revised Manuscript Received October 30, 2002

ABSTRACT: Progression through S phase of the eukaryotic cell cycle is regulated by the action of the cyclin dependent protein kinase 2 (CDK2) in association with cyclin A. CDK2/cyclin A phosphorylates numerous substrates. Substrate specificity often employs a dual recognition strategy in which the sequence flanking the phospho-acceptor site (Ser.Pro.X.Arg/Lys) is recognized by CDK2, while the cyclin A component of the complex contains a hydrophobic site that binds Arg/Lys.X.Leu ("RXL" or "KXL") substrate recruitment motifs. To determine additional sequence specificity motifs around the RXL sequence, we have performed X-ray crystallographic studies at 2.3 Å resolution and isothermal calorimetry measurements on complexes of phospho-CDK2/cyclin A with a recruitment peptide derived from E2F1 and with shorter 11-mer peptides from p53, pRb, p27, E2F1, and p107. The results show that the cyclin recruitment site accommodates a second hydrophobic residue either immediately C-terminal or next adjacent to the leucine of the "RXL" motif and that this site makes important contributions to the recruitment peptide recognition. The arginine of the RXL motif contacts a glutamate, Glu220, on the cyclin. In those substrates that contain a KXL motif, no ionic interactions are observed with the lysine. The sequences N-terminal to the "RXL" motif of the individual peptides show no conservation, but nevertheless make common contacts to the cyclin through main chain interactions. Thus, the recruitment site is able to recognize diverse but conformationally constrained target sequences. The observations have implications for the further identification of physiological substrates of CDK2/cyclin A and the design of specific inhibitors.

Progression through the cell cycle is controlled by the sequential activities of different cyclin-dependent protein kinases that require association with their respective cyclins and phosphorylation for activation (reviewed in refs *1*−*3*). Cells respond to mitogenic signals through activities initiated by CDK4 and CDK6 whose association with D-type cyclins may be promoted by members of the $p21^{Cip1}$ class of CDK inhibitors (CKIs). A major target of these CDKs is the tumor suppressor protein, pRb, whose phosphorylation leads to relief of its transcriptional repression of the E2F family of transcription factors (*4*, *5*) and results in expression from E2F responsive promoters such as that for cyclin E. Cyclin E in association with CDK2 initiates events that drive cells from G1 to S phase (*6*, *7*). Levels of cyclin A rise at the G1/S boundary and, in association with CDK2, are responsible for S phase progression. CDK2/cyclin A phosphorylates a wide range of substrates; these include the tumor suppressor pRb and the related proteins p107 and p130, transcription factors such as MybB, ID2, ID3, and p53 (*8*−*11*), and CDC6, a protein involved in the formation of the prereplication complex (*12*, *13*). CDK2/cyclin A also phosphorylates the heterodimeric transcription factor E2F/DP (*14*), resulting in loss of DNA binding by the complex and thus inactivation of transcription, an important signal for promoting exit from S phase. Cyclin A levels remain high through G2 but as cells enter M phase, cyclin A is degraded through the action of the anaphase promoting complex. Cyclin B then becomes active, and, in association with CDK1, promotes the completion of M phase.

The generic substrate sequence recognized by CDK2/cyclin A is S/TPXK/R, where S or T are the phospho-acceptor residues, X is any amino acid, and K/R denote a preference for a basic residue (*15*−*17*). A decade ago, the two pRb related proteins, p107 and p130, and E2F were found to form stable stoichiometric complexes with either CDK2/cyclin E or CDK2/cyclin A (*18*−*21*). Cyclin binding was found to utilize a motif termed the cy or RXL motif that also occurs in the CDK2 inhibitors $p21^{Cip1}$ and $p27^{Kip1}$ (*22*, *23*). Many other CDK2 substrates, such as pRb (*24*, *25*), p53 (*11*), E2F1 (*14*, *26*), human papilloma virus (HPV) replication factor E1 (*27*), $p220^{NPAT}$ (*28*), CDC6 (*29*, *30*), endomexin (*31*, *32*), and HIRA (*33*) also contain this interaction motif at a site that is remote from the phospho-

[†] This work was supported by the Medical Research Council and the Biotechnology and Biological Sciences Research Council.

[‡] Coordinates have been deposited as Protein Data Bank entries 1h24 (E2F peptide complex), 1h25 (pRb peptide complex), 1h26 (p53 peptide complex), 1h27 (p27 peptide complex) and 1h28 (p107 peptide complex).

* To whom correspondence should be addressed. Tel: 00 44 (0)-1865 275365. Fax: 00 44 (0)1865 510454. E-mail: louise@biop.ox.ac.uk.

[§] University of Oxford.

[¶] National Institute for Medical Research.

10.1021/bi0268910 CCC: $22.00
Published on Web 12/07/2002

Site		- 7	- 6	- 5	- 4	- 3	- 2	- 1	0	+ 1	+ 2	+ 3			Residues
E2F	G	R	P	P	V	K	R	R	L	D	L	E	T	D	84-97
P53		S	T	S	R	H	K	K	L	M	F	K			376-386
pRb		P	P	K	P	L	K	K	L	R	F	D			868-878
E2F				P	V	K	R	R	L	D	L	E			97-95
p27		K	P	S	A	C	R	N	L	F	G	P			25-35
p107		A	G	S	A	K	R	R	L	F	G	E			653-663

FIGURE 1: Recruitment peptide sequences used in crystallographic binding studies with pCDK2/cyclin A. The RXL motif is shown shaded.

acceptor residue. RXL containing peptides are effective inhibitors of the activity of CDK2/cyclin A against RXL containing substrates and such peptides derived from E2F preferentially induced transformed cells, whose E2F transcriptional machinery had been deregulated, to undergo apoptosis relative to nontransformed cells (*34*). These studies have provided a rational for the development of CDK2/cyclin A antagonists based on the RXL motif as antineoplastic agents.

Structural studies on complexes of phospho-CDK2/cyclin A with the $p27^{Kip1}$ inhibitor (*35*) and with a peptide from p107 (*36*) have shown that the RXL recognition site is located at an exposed, hydrophobic site on the cyclin A molecule, that is conserved in cyclins A, B, D, and E (*37*). The recruitment site is some 40 Å from the catalytic site (*36*) of CDK2. Mutation of residues within the hydrophobic patch on cyclin A eliminates efficient phosphorylation of substrates that include RXL motifs but not certain CDK2 substrates, such as histone H1, that do not contain this motif (*38*). In some instances, although there is no stable association of the substrate with CDK2, the integrity of the RXL motif still appears critical for efficient phosphorylation of target substrates such as pRb and p53 (*11*, *38*, *39*). Paradoxically, stronger physical association between the CDK/cyclin and the substrate does not necessarily lead to a more efficient phosphorylation than a weaker interaction (*26*). One of the roles of the RXL motif may be to make an otherwise poor substrate a good substrate (*40*).

Examination of the sequences around the RXL motif from a number of key substrates shows variation in sequence and in position of the RXL motif with respect to the site of phosphorylation. To better understand the factors involved in the recognition of the RXL motif by cyclin A we have co-crystallized phospho-CDK2/cyclin A (pCDK2/cyclin A)[1] in complex with a peptide from E2F1 (residues 84−97). We have also carried out a systematic study of five peptides from pRb, p107, E2F1, p27, and p53 (Figure 1), using both crystallography and isothermal titration calorimetry to characterize this important interaction.

EXPERIMENTAL PROCEDURES

Peptides. Peptides corresponding to residues 376−386 and 381−386 for p53; 870−878 and 873−878 for pRb; 25−35 and 30−35 for p27; 84−97, 85−95, and 90−95 for E2F; and 653−663 and 658−663 for p107 were synthesized by Dr G. B. Bloomberg, Department of Biochemistry, University of Bristol.

Bacterial Expression and Purification of pCDK2/Cyclin A3. Human phospho-CDK2 (phosphorylated at Thr160) was obtained from coexpression of human GST-CDK2 and *Saccharomyces cerevisiae* GST-Cak1, encoded in a pGEX vector as bicistronic construct, in *Escherichia coli* B834-(DE3)pLysS cells (*36*). Untagged human cyclin A3 (residues 174−432) was expressed using a pET21d vector in *E. coli* B834(DE3) pLysS cells. Purification of the pCDK2/cyclin A complex was achieved as previously described (*36*).

Crystallization and Structure Determination of pCDK2/Cyclin A/E2F (Residues 84−97) Peptide. Co-crystallization of the pCDK2/cyclin A/E2F peptide (residues 84−97) was performed using the hanging drop vapor diffusion method from solutions containing equal volumes of pCDK2/cyclin A solution (concentration 10 mg mL^{-1}) in 50 mM HEPES, pH 6.5, 300 mM NaCl, 1 mM EDTA, 0.7 mM BME, 1 mM AMPPNP, 1 mM ATP, 5% glycerol, 0.5 mM E2F peptide, and reservoir solution containing 1.1 M ammonium sulfate, 100 mM HEPES, pH 6.4. X-ray data to 2.4 Å were collected from crystals cryoprotected by mother liquor containing 20% glycerol at 100 K. The crystals are space group *C*2, unit cell dimensions $a = 51.8$ Å, $b = 74.6$ Å, $c = 181.8$ Å, $\beta = 122.30°$. Data were collected at SRS, Daresbury and ESRF, Grenoble and processed using HKL-suite and CCP4 programs (*41*, *42*). The data comprising 894 782 reflections reduced to a unique set of 109 955 reflections in the resolution range 18 to 2.4 Å (98.5% complete) with Rsym = 0.058. The structure was solved by molecular replacement using the coordinates of 1QMZ (*36*) (with ligand atoms and waters removed) as a search model. The structure was refined with REFMAC to give a crystallographic R-value of 0.221 and free R-value of 0.291. The RMSD in bond length and bond angles were 0.020 Å and 2.4°, respectively, for 14 980 atoms with overall B factor of 39 $Å^2$. The asymmetric unit contained three molecules of the CDK2/cyclin A/E2F peptide complex. The description of the contacts is based on the analysis of the complex designated by the chain identifiers A(pCDK2), B(cyclin A), and C(E2F peptide).

Crystallization for Peptide Soak Experiments with p53, pRb, p27, E2F, and p107 Peptides. Crystallization of pCDK2/cyclin A was achieved using the sitting drop method. Equal volumes (1 μL) of pCDK2/cyclin A solution (concentration of 10 mg ml^{-1}) in 10 mM HEPES, pH 7.4, 150 mM NaCl, 3.4 mM EDTA, 0.01% azide, 0.01% monothioglycerol were mixed with 1 μL of reservoir solution containing 0.8 M KCl, 1.2 M $(NH_4)_2SO_4$, 100 mM HEPES pH 7.0. Attempts to co-crystallize pCDK2/cyclin A with peptides were not successful. The structures of the peptides in complex with pCDK2/cyclin A were obtained by soaking preformed crystals in peptide solutions made up in reservoir solution with the following conditions: p53 peptide: 1 mM for 10 min; pRb peptide: 1 mM for 10 min; p27 peptide: 1 mM for 2.75 min; E2F peptide; 1 mM for 3 min. Crystals were cryoprotected by immersing for less than 1 s in 8 M formate in water before placing in the cryostream of liquid nitrogen at 100 K.

The crystals grown in the presence of $(NH_4)_2SO_4$ are chunkier than previous crystals grown in the presence of Li_2SO_4 and hence were preferred for diffraction experiments. The crystals belong to space group $P2_12_12_1$ and contain two pCDK2/cyclinA molecules per asymmetric unit. In one pCDK2/cyclin A molecule, the recruitment site (on the B

[1] Abbreviations: pCDK2, phospho(Thr160)cyclin-dependent kinase 2; HEPES, *N*-(2-hydroxyethyl)piperazine-*N*′-2-ethanesulfonic acid; ITC, isothermal calorimetry.

Table 1: Summary of Crystallographic Data for pCDK2/Cyclin A Recruitment Peptide Complexes

substrate	p53	pRb	p27	E2F	p107
peptide[a]	ST**SRHKKLMFK**	P**PKPLKKLRFD**	KPSAC**RNLFGP**	**PVKRRLDLE**	A**GSAKRRLFGE**
synchrotron	ESRF BM14	ESRF14.1	ESRF 14.2	ESRF 14.1	ESRF 14.4
soak conditions	1 mM peptide for 10 min	1 mM peptide for 10 min	1 mM peptide for 2.75 min	1 mM peptide for 3 min	1 mM peptide for 10 min
space group	$P2_12_12_1$	$P2_12_12_1$	$P2_12_12_1$	$P2_12_12_1$	$P2_12_12$
unit cell (Å)	73. 7 134.0 147.9	73.9 134.1 149.3	73. 7 134.0 147.9	73.6 133.6 147. 9	149.5 162.5 71.4
resolution (Å);	2.24	2.5	2.2	2.5	2.8
(highest range)	(2.36−2.24)	(2.59−2.50)	(2.32−2.2)	(2.56−2.50)	(2.95−2.8)
no reflections	223072	252831	181975	124102	92651
no unique	63733	52141	63569	48503	41507
multiplicity	3.3 (1.8)	4.8 (4.6)	2.6 (2.6)	2.6 (2.4)	2.2 (2.1)
I/σ_I	9.1 (1.3)	6.2 (1.7)	6.4 (1.4)	8.8 (1.7)	2.8 (1.2)
completeness %	96.5 (75.5)	100 (100)	98.7 (98.7)	95.6 (94.4)	95.7 (97.8)
Rsym	0.069 (0.442)	0.092 (0.439)	0.073 (0.399)	0.062 (0.443)	0.166 (0.617)
refinement (Å)	35−2.2	20−2.5	29.6−2.2	100−2.5	29.6−2.8
protein atoms	8831	8845	8949	8969	9036
waters	101	192	232	232	37
Rconv	0.216	0.238	0.232	0.212	0.266
Rfree	0.268	0.296	0.261	0.270	0.327
mean B factor					
protein (Å^2)	42.6	54.6	47.8	55.7	34.5
peptide (Å^2)	58	53.7	46.2	62	47.5
rmsd bonds (Å)	0.017	0.012	0.008	0.018	0.014
rmsd angles (°)	1.70	1.38	1.19	1.85	1.84

[a] Bold indicates residues visible in density.

chain cyclin) is readily accessible with no lattice contacts in the vicinity. In the other pCDK2/cyclin A molecule, the recruitment site (on the D chain cyclin) is blocked by a leucine residue (Leu96) from a symmetry-related C chain (pCDK2). Lattice contacts also affect the C (pCDK2) subunit from residues 236−250 which are in close contact with the A (pCDK2) subunit C-terminal residues 294−296. These residues are disordered and were omitted from the refined structures. The disorder does not affect recruitment peptide binding. The crystals became fragile when soaked in the recruitment peptides. We tested if the presence of nucleotides or related compounds bound at the catalytic site could increase the stability of the crystals. No significant effects were found. For two of the peptide complexes (pRb and E2F) the crystals contained 1 mM AMPPNP with no Mg^{2+}. For the p53 peptide complex, the crystals contained 1 mM methyloxypurine inhibitor, a relatively weak nucleotide inhibitor that exhibits 36% inhibition of CDK2/cyclin A activity at 100 μM. It was found that AMPPNP diffused out of the crystals in the absence of Mg^{2+} on soaking the crystals in the peptide solutions leaving an empty nucleotide triphosphate site but that the methyloxypurine inhibitor remained bound at the ATP binding site.

Attempts to soak the crystals grown in the presence of $(NH_4)_2SO_4$ in the p107 peptide solution were not successful. Low concentrations (0.1 mM for 10 min) or short soaks at higher concentrations (1 mM for 2 min) resulted in no binding, while higher concentrations or longer soaks resulted in crystal cracking. We therefore used crystals grown in the presence of 1.0 M Li_2SO_4 as precipitant (*36*) in which the recruitment sites on both the cyclin molecules in the asymmetric unit are accessible. These crystals are platelike and tend to grow to smaller dimensions than those grown in the presence of $(NH_4)_2SO_4$. Crystals were soaked in a solution containing 1 mM p107 peptide in 1.0 M Li_2SO_4, 100 mM HEPES pH 7.0 for 10 min. The crystals were cryoprotected with 8 M formate before data collection.

Data were collected at ESRF, Elettra, and SRS. Data were processed using MOSFLM (*43*) and CCP4 programs (*42*). The structures were solved by molecular replacement (*44*) using as starting model the coordinates for the pCDK2/cyclin A/p107 hexapeptide complex (PDB code 1QMZ) (*36*) from which the peptide, AMPPNP and water molecules had been removed. The resulting solution was refined by rigid body refinement in REFMAC (*45*) using data of increasing resolution and rigid bodies of decreasing size followed by five cycles of maximum likelihood refinement in REFMAC. At this stage inspection of the SigmaA weighted $2F_o-F_c$ and F_o-F_c electron density maps with O (*46*) indicated binding of peptide at the recruitment site of the B cyclin subunit for the $(NH_4)_2SO_4$ crystals and both the B and D cyclin subunits for the Li_2SO_4 crystals. The peptide atoms were added to the structure and refinement continued with REFMAC using a weighting of 0.05 for X-ray to stereochemical restraints and with iterative rebuilding in O. Water molecules were included using REFMAC/ARP (*47*). Refinement statistics for the recruitment peptide complexes are summarized in Table 1. For p53, the first two residues from the N-terminus do not have density and for pRb the N-terminal proline is without density. For p27, five residues from the N-terminus are without density. We consider that this is a consequence of diffusion of a high affinity peptide into the ammonium sulfate crystal form where it competes for a lattice contact (see above). In the description of contacts, we refer to the previous cocrystal structure of the p27 complex (*35*). For E2F, where a nine-mer was used, all nine residues are observed. For p107, the N-terminal alanine is not observed in one of the subunits, and the three N-terminal residues are not observed in the other subunit. In the previously published co-crystallized structure of pCDK2/cyclin A with the p27 peptide residues 25−93 (*35*) and in the E2F (residues 84−97) complex described above, the N-terminal residues are visible but make no strong interactions with the cyclin.

Isothermal Calorimetry. The binding constants of a series of peptides for the cyclinA/CDK2 complex were determined by isothermal titration calorimetry (ITC) using a MicroCal Omega VP−ITC machine (MicroCal). For each series of experiments ITC measurements were carried out against the same preparation of pCDK2/cyclin A. Protein stored at −80 °C was thawed and dialyzed overnight at 4 °C against 2 L of buffer containing 40 mM Hepes pH 7.0, 200 mM NaCl, 1 mM TCEP. After dialysis, the protein was filtered through a Whatman Anatop 0.02 micron filter and then diluted to a final concentration of 10 μM with dialysis buffer. The protein sample was assessed, prior to dilution, by dynamic light scattering using a Dyna Pro-801 machine from Protein Solutions Inc. Peptide samples were dissolved in dialysis buffer and then desalted using a PD-10 spin column (Amersham Pharmacia Biotech AB). Only monodisperse samples were found to be suitable for determination of reliable binding measurements. The ITC measurements were carried out at 25 °C using 10 μm cyclinA/cdk2 in the calorimeter and 110 μM peptide in the injection syringe. After subtraction of the dilution heats, calorimetric data were analyzed using the evaluation software MicroCal Origin v5.0 (MicroCal Software). For these experiments, independent measurements were made at least twice for each peptide. There was less than 15% variation between readings.

RESULTS

Structure of the pCDK2/Cyclin A/E2F Peptide Complex. A 14-residue synthetic peptide whose sequence was derived from E2F-1 (residues 84−97) was co-crystallized with pCDK2/cyclin A and the structure solved at 2.4 Å resolution. The crystals belong to the space group *C*2 and contain three copies of the complex in the crystallographic asymmetric unit. The peptide is bound at the previously identified recruitment site on cyclin A and makes contacts solely with the cyclin A (Figure 2a). The structures of the three copies of the E2F-1 peptide were similar in the core regions (residues 86−94) but with some significant differences in conformation at the immediate N-terminus and over the last three residues at the C-terminus where there are few interactions between the peptide and the protein. In all three copies, there are identical contacts between the leucine (Leu-92) of the RXL motif and the hydrophobic pocket on the cyclin. We introduce a nomenclature in which the leucine site of the "RXL" motif is denoted as the P0 site and residues on the target peptide N-terminal to this are denoted P-1, P-2, etc., and C-terminal P+1, P+2, etc.

In the crystal structures of $p27^{Kip1}$ and p107 peptides bound to pCDK2/cyclin A, the phenylalanine residue of the RXLF motif is involved in significant van der Waals contacts with the cyclin. In E2F, the corresponding residue following the RXL motif is an aspartic acid (Figure 1). We were interested therefore to compare the structure of the bound E2F peptide with that of the $p27^{Kip1}$ and p107 complexes to understand how the recruitment site accommodates such a marked difference in sequence. Unlike the phenylalanine residue in the two previous structures, E2F−Asp93 (P+1) is oriented away from the cyclin and makes no interactions with it. Instead, the next residue in the E2F peptide, E2F−Leu94 (P+2), occupies a similar position to the phenylalanine at the P+1 position in the $p27^{Kip1}$ and p107 structures (Figure 2b). E2F−Leu94 (P+2) makes extensive van der Waals

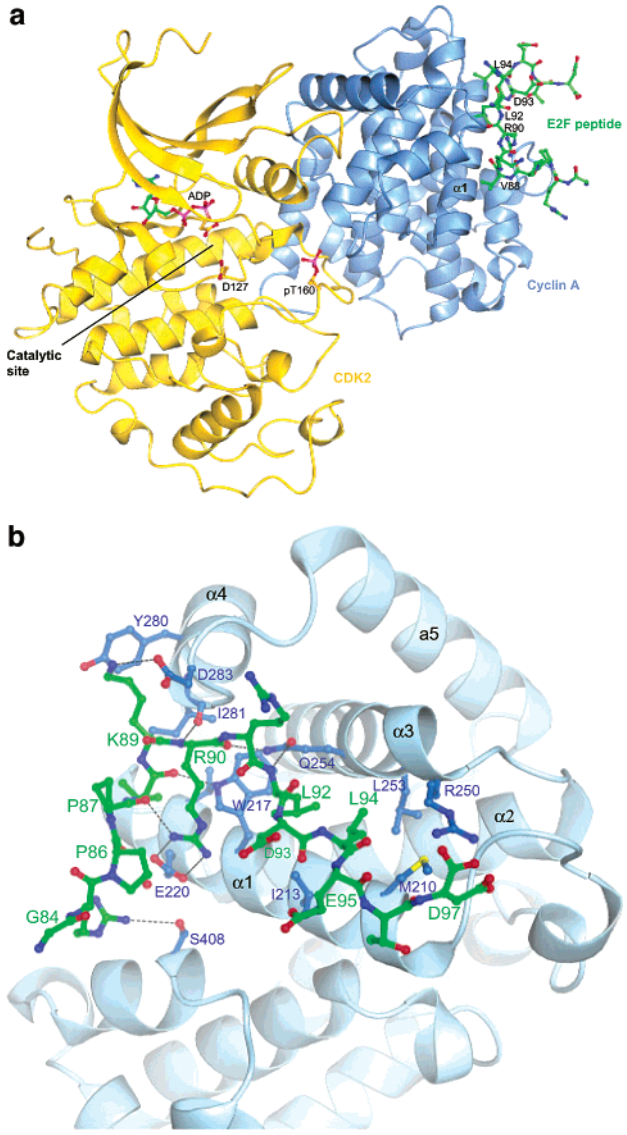

FIGURE 2: The location of the E2F peptide (residues 84−97) on the pCDK2/cyclin A complex. pCDK2 is shown in yellow, cyclin A in dark blue, and the E2F peptide in ball-and-stick representation with carbon atoms green. (a) Overall schematic representation. The E2F peptide binds on the surface of the cyclin A molecule. Also shown are the pCDK2 phospho-Thr160 residue and the catalytic site, which is marked by the binding of ADP and the catalytic aspartate, Asp127. (b) Details of the contacts made by the E2F peptide and residues on cyclin A. For further details see text. This figure and the other figures were prepared with Aesop (M. E. M. Noble, unpublished work).

contacts with the cyclin as well as with E2F−Leu92 (P0) and by this means acts as a mimic for the phenylalanine at P+1 in $p27^{Kip1}$ and p107.

Residues 86−95 of the E2F peptide bind in an extended conformation, interrupted by an α-helical conformation for E2F−Val88 (P-4 site). The peptide docks against the cyclin α1 helix with contacts from the cyclin α3 and α4 helices of the N-terminal cyclin box fold (Figure 2b). The side chain of E2F−Arg85 (P-7) interacts with the side chain hydroxyl of cyclin Ser-408 while the next three residues make hydrogen bonds via their main chain carbonyl oxygens; E2F−Pro-86 (P-6) interacts through a water molecule with the OE2 of cyclin−Glu220; E2F−Pro87 (P-5) makes an intramolecular hydrogen bond with the side chain of E2F−Arg90 (P-2) and E2F−Val88 (P-4) main chain oxygen

interacts with the NE1 of cyclin−Trp217. The contact from E2F−Val88 is made possible by the α turn at this residue. The following residue on the peptide, E2F-Lys89 (P-3), makes an exposed salt bridge through the interaction of its side chain with that of cyclin−Asp283. E2F−Arg90 (P-2), the arginine of RXL, makes two main chain hydrogen bonds. It interacts via its nitrogen with the main chain carbonyl oxygen of cyclin−Ile281 and through its carbonyl oxygen to the side chain of cyclin−Gln254. The side chain of Arg90 makes a bidentate salt bridge with cyclin−Glu220. The main chain nitrogen of E2F−Leu92 (P0) hydrogen bonds to the side chain of cyclin−Gln254, while its side chain fits into a largely hydrophobic pocket making extensive van der Waals. As described above, E2F−Asp93 (P+1) does not interact with the cyclin but E2F−Leu94 (P+2) does. Beyond this point in the peptide chain there are few interactions with the protein and these tend to be different among the three copies of the complex in the asymmetric unit.

Structures of Further pCDK2/Cyclin A/Peptide Complexes. Following the previous result, we made a systematic study of the structures, and thermodynamics of binding, for five different peptides from important pCDK2/cyclin A substrates in which the length of the peptide was restricted to the core region (Figure 1). As we were not successful in co-crystallizing these peptides with pCDK2/cyclin A, the crystallographic analysis was carried out by diffusing peptides into preformed crystals. We are satisfied with the validity of this approach because co-crystallized and diffused peptide complex structures of E2F and p27 peptides show nearly identical structures for the residues in common. Portions of the electron density maps in the vicinity of the bound peptides for the five complexes are shown in Figure 3.

From superposition of the five recruitment peptide complexes, it is readily apparent that the position of the leucine of the RXL motif, (P0), is conserved in all of the structures (Figure 3). In the p27 and p107 peptide complexes, the site at P+1 is occupied by a phenylalanine that makes extensive contacts to the cyclin and to the preceding leucine (P0). In contrast, for the p53, pRb, and E2F peptides, it is the residue at the P+2 position (p53−Phe385, pRb−Phe877, and E2F−Leu94) that occupies this site and the intervening P+1 residue (p53−Met384, pRb−Arg876, and E2F−Asp93) is oriented out into solution. This difference in peptide binding is accomplished by an α conformation at Leu (P0) in the p27 and p107 complexes in contrast to a β conformation at this site for p53, pRb, and E2F. Thus, in addition to the conserved P0 leucine on the target peptide, there is also a conserved nonpolar residue at either the P+1 or the P+2 position. Display of the hydrophobic potential on the van der Waals surface of the cyclin shows that the site that accommodates residues P0 and either P+1 or P+2 has complementarity both in shape and in nonpolar character to these nonpolar residues (Figure 4). The leucine (P0) site makes between 12 and 19 van der Waals interactions in the different peptide complexes with nonpolar groups on the cyclin contributed mostly by residues Trp217 and Gln254 (Supporting Information). The 13−24 nonpolar contacts made by the phenylalanine in the P+1 position in the p107 and p27 peptide complex structures include contributions from Met210 and Leu253 and some contributions from residues Ile213, Arg250, and Gln254. In the p53, and pRb peptide complexes the P+2 residue, p53−Phe385, and pRb−Phe876, make 21 and 22 contacts, respectively, while E2F−Leu94 makes eight contacts. Beyond the P+2 site, there is a variability in the conformations adopted by the different peptides (Figure 3).

The residues N-terminal to the leucine at P0 show a similar conformation from sites P-1 to P-4 for all five peptide complexes, and the main chain hydrogen bond interactions are as previously described for the E2F co-crystallized complex. Importantly, the main chain oxygen at P-2 and the main chain nitrogen at P0 make hydrogen bonds to cyclin−Gln254 OE1 and Gln254 NE2, respectively, indicating a constraint on the conformation of the peptide in the P-2 to P0 positions. This constraint is reinforced by a hydrogen bond between the main chain nitrogen at P-2 and the main chain carbonyl oxygen at cyclin−Ile281. The P-4 site is characterized by a conserved hydrogen bond from the main chain oxygen to the side chain nitrogen of cyclin−Trp217 that is achieved by a conserved conformation of the peptides in this region (Supporting Information). Beyond the P-4 site the conformations of each of the peptides differ.

In all five peptides, there is a polar residue at the P-1 position. For p27 and p107, this side chain (p27−Asn31 and p107−Arg659) points into solution but makes an intramolecular hydrogen bond as discussed previously (*36*). For three of the peptides, p53, pRb, and E2F, the P-1 site is occupied by a basic residue (p53−Lys382, pRb−Lys874, and E2F−Arg91). These residues make no contact with the cyclin, although there is the possibility of a long polar contact (>3.4 Å) to the main chain oxygen of Thr282 of the cyclin.

The original identification of the "RXL" motif would appear to argue for an important role for the arginine residue at the P-2 site in three of the peptide complexes (p27−Arg30, E2F−Arg90, and p107−Arg658). In these structures, this arginine makes an ion pair with the carboxylate side chain group of cyclin−Glu220. There are some differences in the length and geometry of these interactions between the complexes formed by co-crystallization or diffusion. A possible explanation for the longer contact distances seen in the diffused peptide complex structures is that these crystals were cryoprotected with 8 M formate, albeit for less than 1 s, while the crystals of the co-crystallized complexes were cryoprotected with glycerol. It could be that the more nonpolar solvent, glycerol, produces less distortion of the ionic interactions than the high ionic strength solvent, formate. For the p53 and pRb complexes, the P-2 residue is lysine and not arginine, and in both cases the lysine residue makes no salt bridge interaction with the cyclin. There are also fewer van der Waals contacts from the aliphatic moiety of the side chain with the cyclin (6 in p53 and 3 in pRb). In pRb, there is no support from the density for a contact to Glu220, although such a contact would be possible through changes in torsion angles of the lysine side chain. In the p53 peptide complex, the lysine side chain is disordered. It appears that under our experimental conditions there is little incentive for a lysine side chain to make an external ion pair interaction with cyclin−Glu220.

In both E2F and p107, the P-3 residue is lysine. In the E2F peptide, the lysine NZ forms an ionic contact with the carboxyl side chain of cyclin−Asp283 (3.3 Å), while in the p107 complex the equivalent atoms are slightly further apart (3.7 Å). These lysine residues make a significant number of

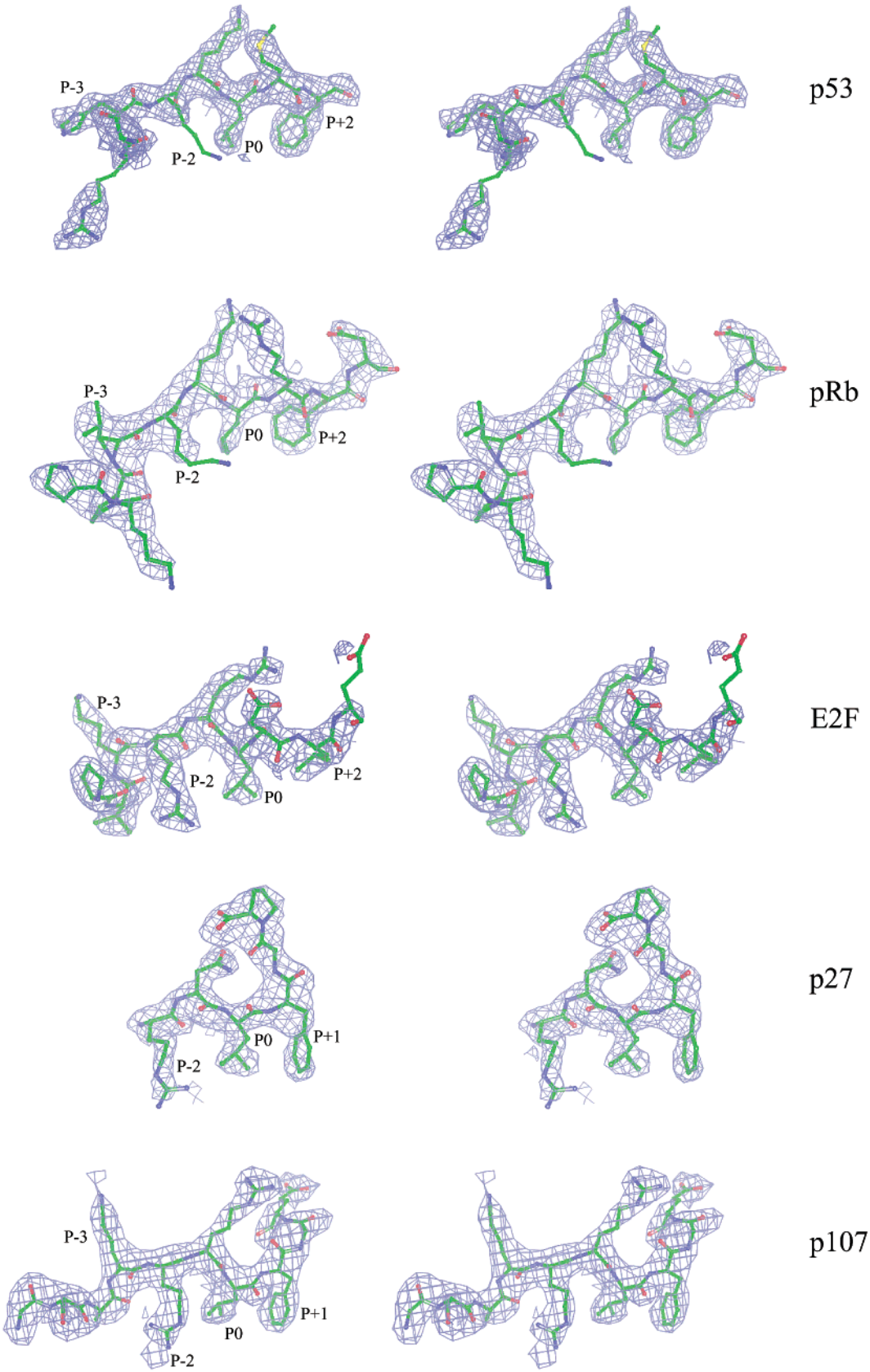

FIGURE 3: Stereoviews of electron density maps in the vicinity of the peptides showing the conformation of the five recruitment peptides in complex with pCDK2/cyclin A. The $2F_o-F_c$ maps are contoured at a level corresponding to 1 σ. Each map is displayed so that the leucine residues at P0 in each peptide are in vertical alignment. The lysine residues at sites P-2 in the p53 and pRb peptide complexes have poor electron density. The hydrophobic residues at the P+2 site in the p53, pRb and E2F peptide complexes occupy a similar site adjacent to the leucine in the P0 site. In the p27 and p107 peptide complexes, this site is taken by the phenylalanine at P+1. Although the recruitment site on the cyclin A (chain B) is open and is able to accommodate all 11 residues of the peptides, in several of the complex structures formed by diffusion of peptides into preformed crystals, some residues at the peptide N-terminus are not supported by density (see Experimental Methods).

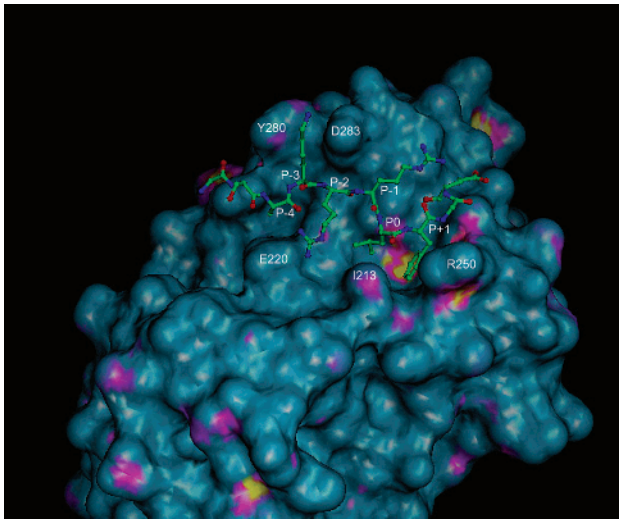

FIGURE 4: The van der Waals surface of cyclin A in the vicinity of the recruitment peptide binding site with the hydrophobic potential calculated by GRID (*52*, *53*). The deepest hydrophobic potential is colored yellow, the medium is magenta, and the neutral surface is gray-blue. The position of the p107 peptide is shown for reference. The leucine at P0 and the phenylalanine at P+1 dock into the most hydrophobic site on the surface.

nonpolar van der Waals contacts (16 contacts in both complexes) with nonpolar side chains from the cyclin molecule, including Tyr280 and Asp283 and Ile281 (Figure 4). In the other three complexes (p53, p27, and pRb), there are also a number of contacts from the side chain at P-3 (p53-His380: 7 contacts; pRb-Leu872: 10 contacts; and p27-Cys29: 8 contacts). Despite the lack of conservation of sequence at this position, the structures suggest that residues at the P-3 site contribute to binding. The partially buried P-4 site also accommodates a variety of side chains (p53−Arg379, pRb−Pro871, p27−Ala28, E2F−Val88, and p107−Ala656), which make a number of nonpolar van der Waals interactions (from 4 for p53 to 13 for p27). No contacts are made at the P-5 site in the p53 and pRb peptides but in p27 the serine at this site contacts the side chain of cyclin−Glu220, in p107 the serine main chain also contacts the side chain of cyclin−Glu224, and in E2F there is an internal hydrogen bond between proline main chain oxygen and the arginine side chain at the P-2 position.

Analysis for Conformational Changes. The structures of the cyclin A molecule in the five 11-mer peptide complexes and in the E2F co-crystallized complex were compared with an unliganded cyclin A molecule in a pCDK2/cyclin A complex (coordinates 1qmz). As previously observed the cyclin is rigid. The rms deviations of Cα coordinates compared with unliganded cyclin A for the whole of the cyclin A molecule ranged from 0.25 to 0.46 Å. The largest value was for the co-crystallized E2F complex cyclin subunit B where there was a slight shift in residues 270−274 of the cyclin molecule. The estimated standard deviation in coordinates derived from the free *R* value is about 0.35 Å. Hence, the analysis indicates that there were no significant changes in the cyclin between bound and unbound state. Visual inspection of each of the subunits confirmed this.

Comparison with an unliganded pCDK2 structure in a pCDK2/cyclin A complex (coordinates 1jst) showed slightly greater variation in rms differences in Cα atoms that ranged from 0.54 to 0.59 Å for the complexes with the E2F (9-mer), pRb, p53, p27 peptides to 0.71 Å for the co-crystallized E2F peptide pCDK2/cyclin A complex and the p107 peptide complex. Examination of the regions of greatest displacement showed that these all occurred on regions of the surface of the molecule (including part of the glycine rich loop residues 13−16) that were not well ordered. There were no significant changes at the catalytic site. It is concluded that binding of peptides at the recruitment site leads to no significant conformational changes at the catalytic site.

Table 2: Isothermal Calorimetry Results for Recruitment Peptides Bound to pCDK2/Cyclin A[a]

		binding constant (μm)	
protein	sequence	11-mer	6-mer
p53	STSRH**KKLMFK**	2.9	2.9
pRb	PPKPL**KKLRFD**	1.8	2.3
p27	KPSAC**RNLFGP**	0.9	2.5
E2F[b]	PVK**RRLDLE**	0.5	7.9
p107	AGSAK**RRLFGE**	0.3	2.4

[a] Residues in bold are the sequences for the short peptide versions. The "RXL" motif is underlined for each sequence. [b] For the E2F peptide the longer version of the peptide contained 9 instead of 11 residues.

Isothermal Calorimetry of Binding Constants. The binding constants for the five recruitment peptides were measured by isothermal titration calorimetry (ITC) (Table 2). Two versions of the peptide were synthesized and assessed for each of the five targets under study; a short version of six residues and a longer version of 11 residues. The most striking feature from these data is the small difference in binding constant among any of the five different types of the 11-residue peptide. The binding constants vary from 0.3 μM for the p107 peptide to 2.9 μM for the p53 peptide. The largest difference is a factor of 10 corresponding to a relative difference in free energy of only 5.6 kJ mol^{-1}. Moreover, the binding constants observed for the six-residue version of these five peptides are all, essentially, the same with values between 2.3 and 2.9 μM with the exception of the E2F peptide for which the binding constant of the hexamer is 7.9 μM.

DISCUSSION

The important common features of peptide recognition observed in these five recruitment peptide complexes with pCDK2/cyclin A may be summarized (Figure 5) as follows: (i) the nonpolar pocket that recognizes the leucine at P0 and a nonpolar group either at P+1 or P+2; (ii) the contacts from peptide main chain atoms at sites P0, P-2, and P-4 to polar groups on the cyclin; (iii) van der Waals contacts at both the P-2, P-3, and P-4 sites and (iv) where present, charge/charge contact from Arg at P-2 to Glu220 on the cyclin. These common features suggest a framework that could be used in structure based drug design to provide a potent and selective cyclin-dependent protein kinase inhibitor. Of course, they do not exclude other contacts that could be made by longer sequences. We note that the cyclin A residues that are involved in contacts (Met210, Ile213, Trp217, Leu253, Gln254, Asp283) are conserved in cyclins A, B, D, and E, but that Glu220, although conserved in cyclins A, D, and E, is glutamine in cyclin B.

The comparison of these structures shows that binding is achieved by the combination of hydrophobic contacts,

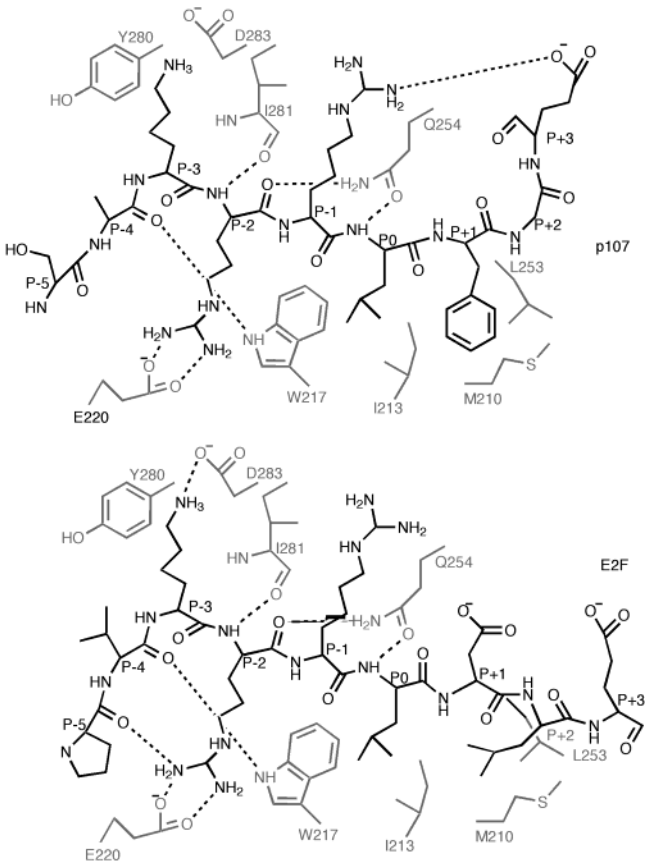

FIGURE 5: A schematic diagram showing the important polar and nonpolar contacts for the complex of pCDK2/cyclin A with the p107 and E2F peptides. The peptide bonds are in black and those of cyclin A in gray. Hydrogen bonds are dotted. The diagram shows the two modes of binding in which either the P+1 residue fills the hydrophobic pocket (p107) or the P+2 residue (E2F).

mediated by the side chains of the peptide, and hydrogen bonds interactions via its main chain. The small differences in binding affinity for the five hexapeptides, as measured by isothermal calorimetry, seem to reinforce this view. As emphasized above, the central feature in target recognition appears to be the leucine of the RXL motif reinforced by a nonpolar residue that is either immediately adjacent or next adjacent to it in the peptide. The structures presented here show how the cyclin binding site is able to accommodate either a charged or hydrophobic residue immediately C-terminal to the RXL motif. Importantly, our structural data have highlighted the role of the hydrophobic residue located at either position P+1 or P+2. Our results also show that there are significant additional van der Waals contacts between the side chains of residues at P-2 and P-3 with the cyclin, although the amino acids at these positions differ among the five target sequences. Thus, the binding site on the cyclin can accommodate a variety of sequences providing that these hydrophobic contacts are largely satisfied. The binding of these different sequences is accomplished within the framework of a conserved peptide backbone conformation prior to the core leucine. Achieving this conformation appears to be facilitated by specific hydrogen bonds between the cyclin and the main chain of the peptide.

The conformation of the peptide from p53 in complex with pCDK2/cyclin A is different from that of the p53 peptide residues 367−388 in complex with Ca^{2+} bound S100B($\beta\beta$) where the corresponding region adopts an α helical conformation (*48*). When free in solution the peptide has no defined structure. It can evidently adopt a structure complementary to the affinity site on the relevant protein using a few side chain interactions as locators.

The p107, p27, and E2F peptides show an increase in affinity as the peptide length is extended from a 6-mer to an 11-mer (9-mer for E2F), while the two peptides, p53 and pRb, do not show such an increase (Table 2). We note that the two lower affinity peptides contain a lysine in place of the arginine of the RXL motif. CDK2/cyclin A has been observed to form stable complexes with p107, p27, and E2F but not with p53 and pRb. Both the structures and the affinity measurements indicate that the arginine makes some contribution to binding, although other residues may be tolerated at this site (*49*). In addition to the ionic interaction with cyclin−Glu220, the role of the arginine may be to assist in locating the residues N-terminal to this site. In the E2F peptide complex, the P-2 arginine side chain contacts the main chain oxygen of the P-5 residue, which may contribute to intramolecular conformational stabilization of the complex, although an equivalent contact is not observed in the other complexes. The arginine residue of the RXL motif enhances the affinity of interaction between target motifs and the cyclin molecule, but our data suggest that this residue can be substituted for lysine at modest cost to the binding affinity. A lysine does not appear to make a salt bridge through its side chain amino group with cyclin−Glu220, but it does make some van der Waals contacts through the alkyl part of its side chain. The observations that different residues at the P-3 and P-4 positions make van der Waals contacts with the cyclin, and that the cyclin binding site makes use of a hydrophobic residue at either P+1 or P+2, suggest a binding motif that may be more extensive than is implied by "RXL". Indeed, we observe a roughly linear relationship between ln Kd and the number of nonpolar contacts made between peptide residues binding to sites −7 to +3 (Supporting Information) with the largest number of contacts made by the high affinity 11-mer p107 peptide (77 contacts) and the fewest (52 contacts) by the low affinity p53 peptide, indicating good correlation between contacts and binding energy. For the six-residue peptides, there is also a reasonable correlation with the exception of the E2F peptide, suggesting, as discussed above, that in this instance the N-terminal residues are significant for producing a high affinity binding.

Two possible explanations have been put forward for the role of the RXL motif in substrate recognition. First that the motif acts to localize the CDK on the substrate in a relatively nonspecific manner, thus increasing the local substrate concentration (*38*). This explanation was supported by experiments in which the cyclin A recruitment site was inactivated by mutagenesis resulting in loss of catalytic activity of the CDK2/cyclin A complex against the substrate p107. When a different recognition site, with the motif LXCXE, was engineered on a surface loop of the mutant cyclin, phosphorylation activity was restored. Likewise, addition of RXL motifs has been observed to increase phosphorylation of otherwise poorly phosphorylated substrates (*14*, *25*). These experiments suggest that localization is sufficient to enhance catalysis and that no special geometrical relationship between the substrate recruitment and catalytic site is required. Second, it has been proposed that there may be a direct path between the catalytic site on CDK2

and the recruitment site on the cyclin (*30*). In support of this proposal, kinetic analysis has shown that, with a CDC6-based synthetic substrate, phosphorylation of the site S^{74}-PXK is dependent on the integrity of R^{94}XL motif. Peptides containing these two motifs with synthetic linkers that have too short a distance between the RXL and the site of phosphorylation were not phosphorylated. Only when the linker peptide mimicked the natural substrate length did phosphorylation occur efficiently. These results support the notion that there must be a minimal distance between the site of phosphorylation and the RXL motif and that substrate recognition could be bipartite. The present structural results cannot distinguish between these possibilities. The variation in position of the N-terminal and C-terminal residues outside the core recognition motifs of the five peptides suggests that a variety of paths could be followed for the substrate between the recruitment site and the catalytic site. Docking sites have been recognized in other protein kinases, especially the MAP kinase family (*50*), as additional determinants of substrate specificity. Recent structural studies (*51*) with p38 have determined the binding site and have highlighted the importance of hydrophobic interactions, as also identified here for the cyclin A recruitment site. The molecular mechanisms of substrate selectivity and enhancement of catalysis by recruitment or docking sites remain to be elucidated.

ACKNOWLEDGMENT

We thank Dr. Jane Endicott for discussions and advice. We thank the beam line scientists at stations BM14, 14.1, 14.2, and 14.4 at ESRF, Grenoble, at SRS, Daresbury, and at ELETTRA, Trieste, for their support in data collection.

SUPPORTING INFORMATION AVAILABLE

Hydrogen bonds and van der Waals contacts for pCDK2/cyclin A peptide complexes. This material is available free of charge via the Internet at http://pubs.acs.org.

REFERENCES

1. Morgan, D. O. (1997) Cyclin-dependent kinases: engines, clocks and microprcessors, *Annu. Rev. Cell. Dev. Biol. 13*, 261−291.
2. Ewen, M. L. (2000) Where the cell cycle and histones meet. *Genes Dev. 14*, 2265−2270.
3. Harper, J. W., and Adams, P. D. (2001) Cyclin-dependent kinases. *Chem. Rev. 101*, 2511−2526.
4. Harbour, J. W., Luo, R. X., Dei Santi, A., Postigo, A. A., and Dean, D. C. (1999) Cdk phosphorylation triggers sequential intramolecular interactions that progressiviely block Rb functions as cells move through G1. *Cell 98*, 859−869.
5. Muller, H., Bracken, A. P., Vernell, R., Moroni, M. C., Christians, F., Grassilli, E., Prosperini, E., Vigo, E., Oliner, J. D., and Helin, K. (2001) E2Fs regulate the expression of genes involved in differentiation, development, proliferation and apoptosis. *Genes Dev. 15*, 267−285.
6. Sherr, C. J., and Roberts, J. M. (1999) CDK inhibitors: positive and negative regulators of G1-phase progression. *Genes Dev. 13*, 1501−1512.
7. Kelly, T. J., and Brown, G. W. (2000) Regulation of chromosome replication. *Annu. Rev. Biochem. 69*, 829−880.
8. Saville, M. K., and Watson, R. J. (1998) The cell cycle regulated transcription factor B-Myb is phosphorylated by cyclin A/CDK2 at sites that enhance its transactivation properties. *Oncogene 17*, 2679−2689.
9. Hara, E., Hall, M., and Peters, G. (1997) CDK2 dependent phosphorylation of Id2 modulates activity of E2A-related transcription factors. *EMBO J. 16*, 332−342.
10. Deed, R. W., Hara, E., Atherton, G. T., Peters, G., and Norton, J. D. (1997) Regulation of Id3 cell cycle function by CDK2-dependent phosphorylation. *Mol. Cell Biol. 17*, 6815−6821.
11. Luciani, M. G., Hutchins, J. R. A., Zheleva, D., and Hupp, T. R. (2000) The C-terminal regulatory domain of p53 contains a functional docking site for cyclin A. *J. Mol. Biol. 300*, 503−518.
12. Petersen, B. O., Lukas, J., Sorensen, C. S., Bartek, J., and Helin, K. (1999) Phosphorylation of mammalian CDC6 by cyclin A/CDK2 regulates its subcellular localisation. *EMBO J. 18*, 396−410.
13. Delmolino, L. M., Saha, P., and Dutta, A. (2001) Multiple mechanisms regulate subcellular localisation of human CDC6. *J. Biol. Chem. 276*, 26947−26954.
14. Dynlacht, B. D., Moberg, K., Lees, J. A., Harlow, E., and Zhu, L. (1997) Specific regulation of E2F family members by cyclin-dependent kinases. *Mol. Cell Biol. 17*, 3867−3875.
15. Minshull, J., Golsteyn, R., Hill, C. S., and Hunt, T. (1990) The A and B cyclin associated kinases turn on and off at different times in the cell cycle, *EMBO J. 9*, 2865−2875.
16. Songyang, Z., Blechner, S., Hoagland, N., Hoekstra, M. F., Piwica-Worms, H., and Cantley, L. C. (1994) Use of an oriented peptide library to determine the optimal substrates of protein kinases. *Curr. Biol. 4*, 973−982.
17. Holmes, J. K., and Solomon, M. J. (1996) A predictive scale for evaluating cyclin dependent kinase substrates. *J. Biol. Chem. 271*, 25240−25246.
18. Ewen, M. E., Faha, B., Harlow, E., and Livingston, D. M. (1992) Interaction of p107 with cyclin A independent of complex formation with viral proteins. *Science 255*, 85−87.
19. Faha, B., Ewen, M., Tsai, L.-H., Livingston, D., and Harlow, E. (1992) Interaction between human cyclin A and adenovirus E1A-associated p107 protein. *Science 255*, 87−90.
20. Lees, E., Faha, B., Dulic, V., Reed, S. I., and Harlow, E. (1992) Cyclin E/CDK2 and cyclin A/CDK2 kinases associate with p107 and E2F in a temporarily distinct manner. *Genes Dev. 6*, 1874−1885.
21. Hannon, G. J., Demetrick, D., and Beach, D. (1993) Isolation of the Rb-related p130 through its interaction with CDK2 and cyclins. *Genes Dev. 7*, 2378−2391.
22. Zhu, L., Harlow, E., and Dynlacht, B. D. (1995) p107 uses a $p21^{CIP1}$-related domain to bind cyclin/cdk2 and regulate interactions with E2F. *Genes Dev. 9*, 1740−1752.
23. Chen, J., Saha, P., Kornbluth, S., Dynlacht, B. D., and Dutta, A. (1996) Cyclin binding motifs are essential for the function of $p21^{cip1}$, *Mol. Cell Biol. 16*, 4673−4682.
24. Adams, P. D., Sellars, W. R., Sharma, S. K., Wu, A. D., Nalin, C. M., and Kaelin, W. G. (1996) Identification of a cyclin-CDK2 recognition motif present in substrates and p21-like cyclin dependent kinase inhibitors. *Mol. Cell Biol. 16*, 6623−6633.
25. Adams, P. D., Li, X., Sellars, W. R., Baker, K. B., Leng, X., Harper, J. W., Taya, Y., and Kaelin, W. G. (1999) Retinoblastoma protein contains a C-terminal motif that targets it for phosphorylation by cyclin-CDK complexes. *Mol. Cell Biol. 19*, 1068−1080.
26. Guida, P., and Zhu, L. (1999) DP1 phosphorylation in multimeric complexes: weaker interaction with cyclin A through the E2F1 cyclin A binding domain leads to more efficient phosphorylation than stronger interaction through the p107 cyclin A domain. *Biochim. Biophys. Res. Commun. 258*, 596−604.
27. Ma, T., Zou, N., Lin, B. Y., Chow, L. T., and Harper, J. W. (1999) Interaction between cyclin-dependent kinases and human papillomavirus replication-initiation protein E1 is required for efficient viral replication. *Proc. Natl. Acad. Sci. U.S.A. 96*, 382−387.
28. Zhao, J., Dynlacht, B., Imai, T., Hori, T.-A., and Harlow, E. (1998) Expression of NPAT, a novel substrate of cyclin E-CDK2, promotes S-phase entry. *Genes Dev. 12*, 456−461.
29. Delmolino, L. M., Saha, P., and Dutta, A. (2001) Multiple mechanisms regulate subcellular localization of CDC6. *J. Biol. Chem. 276*, 26947−26954.
30. Takeda, D. Y., Wohlschlegel, J. A., and Dutta, A. (2001) A bipartite substrate recognition motif for cyclin-dependent kinases, *J. Biol. Chem. 276*, 1993−1997.
31. Ohtoshi, A., Maeda, T., Higashi, H., Ashizawa, S., Yamada, M., and Hatakeyama, M. (1998) β3-endonexin as a novel inhibitor of cyclin A associated kinase. *Biochem. Biophys, Res. Comm. 267*, 947−952.
32. Ohtoshi, A., and Otoshi, H. (2001) Analysis of β3-endonexin mutants for their ability to interact with cyclin A, *Mol. Genet. Genomics 266*, 664−671.

33. Hall, C., MNelson, D. M., Ye, X., Baker, K., DeCaprio, J. A., Seeholzer, S., lipinski, M., and Adams, P. D. (2001) HIRA, the human homologue of yeast Hir1p and Hir2p, is a novel cyclin-cdk2 substrate whose expression blocks S-phase progression. *Mol. Cell. Biol. 21*, 1854−1865.
34. Chen, Y.-N. P., Sharma, S. K., Ramsey, T. M., Liang, L., Martin, M. S., Baker, K., Adams, P. D., Bair., K. W., and Kaelin, W. G. (1999) Selective killing of transformed cells by cyclin/cyclin dependent kinase 2 antagonists. *Proc. Natl. Acad. Sci. U.S.A. 96*, 4325−4329.
35. Russo, A. A., Jeffrey, P. D., Patten, A. K., Massague, J., and Pavletich, N. P. (1996) Crystal structure of the $p27^{Kip1}$ cyclin-dependent-kinase inhibitor bound to the cyclin A-CDK2 complex. *Nature 382*, 325−331.
36. Brown, N. R., Noble, M. E. M., Endicott, J. A., and Johnson, L. N. (1999) The structural basis for specificity of substrate and recruitment peptides for cyclin-dependent kinases. *Nat. Cell Biol. 1*, 438−443.
37. Brown, N. R., Noble, M. E. M., Endicott, J. A., Garman, E. F., Wakatsuki, S., Mitchell, E. P., Rasmussen, B., Hunt, T., and Johnson, L. N. (1995) The crystal structure of cyclin A. *Structure 3*, 1235−1247.
38. Schulman, B., Lindstrom, D. L., and Harlow, E. (1998) Substrate recruitment to cyclin-dependent kinase 2 by a multipurpose docking site on cyclin A. *Proc. Natl. Acad. Sci. U.S.A. 95*, 10453−10458.
39. Driscoll, B., T'ang, A., Hu, Y.-H., Yan, C. L., Fu, Y., Luo, Y., Wu, K. J., Wen, S., Shi, X.-H., Barsky, L., Weinberg, K., Murphree, A. L., and Fung, Y. K. (1999) Discovery of a regulatory motif that controls the exposure of specific upstream cyclin-dependent kinase sites that determine both conformation and growth suppressing activity of pRb. *J. Biol. Chem. 274*, 9463−9471.
40. Leng, X., Noble, M. E. M., Adams, P. D., Qin, J., and Harper, J. W. (2002) Reversal of growth supression by p107 via direct phosphorylation by cyclin D1/cyclin dependent kinase 4. *Mol. Cell. Biol. 22*, 2242−2254.
41. Otwinowski, Z., and Minor, W. (1997) Processing of X-ray diffraction data collected in oscillation mode. *Methods Enzymol. 276*, 307−326.
42. CCP4. (1994) The CCP4 (Collaborative Computational Project Number 4) suite: programmes for protein crystallography, *Acta Crystallogr. D D50*, 760−763.
43. Leslie, A. G. W. (1992) in *Joint CCP4 and ESF-EACMB Newsletter on Protein Crystallography*, Daresbury Laboratory, Warrington.
44. Navaza, J. (1990) AMoRe: an automated package for molecular replacement. *Acta Crystallogr. A50*, 157−163.
45. Murshudov, G. N., Vagen, A. A., and Dodson, E. J. (1997) Refinement of macromolecular structures by the maximum-likelihood method. *Acta Crystallogr. D53*, 240−255.
46. Jones, T. A., Zou, J. Y., Cowan, S. W., and Kjeldgaard, M. (1991) Improved method for building models in electron density maps and the location of errors in these models. *Acta Crystallogr. A47*, 110−119.
47. Lamzin, V. S., and Wilson, K. S. (1993) Automated refinement of protein models. *Acta Crystallogr. D49*, 129−147.
48. Rustandi, R. R., Baldisseri, D. M., and Weber, D. J. (2000) Structure of the negative regulatory domain of p53 bound to S100B($\beta\beta$). *Nat. Struct. Biol. 7*, 570−574.
49. Wohlschlegel, J. A., Dwyer, B. T., Takeda, D. Y., and Dutta, A. (2001) Mutational analysis of the cy motif from p21 reveals sequence degeneracy and specificity for different cyclin-dependent kinases. *Mol. Cell Biol. 21*, 4868−4874.
50. Sharrocks, A. D., Yang, S. H., and Galanis, A. (2000) Docking domains and substrate-specificity determination for MAP kinases. *Trends Biochem. Sci. 25*, 448−453.
51. Chang, C.-I., Xu, B., Akella, R., Cobb, M. H., and Goldsmith, E. J. (2002) Crystal structures of MAP kinase p38 complexed to the docking sites on its nuclear substrate MEF2A and activator MKK3b. *Mol. Cell 9*, 1241−1249.
52. Goodford, P. J. (1985) A computational procedure for determing energetically favourable binding sites on biologically important macromolecules. *J. Med. Chem. 28*, 849−857.
53. Goodford, P. J. (1996) Multivariate characterization of molecules for QSAR, *J. Chemometrics 10*, 107−117.

BI0268910